Embryonic Lethality and Tumorigenesis Caused by Segmental Aneuploidy on Mouse Chromosome *11*

Pentao Liu,*,† Heju Zhang,* Andrew McLellan,* Hannes Vogel§ and Allan Bradley*,†,‡

**Department of Human and Molecular Genetics, †Program in Developmental Biology, ‡Howard Hughes Medical Institute, §Department of Pathology, Baylor College of Medicine, Houston, Texas 77030*

Manuscript received March 6, 1998
Accepted for publication August 10, 1998

ABSTRACT

Chromosome engineering in mice enables the construction of models of human chromosomal diseases and provides key reagents for genetic studies. To begin to define functional information for a small portion of chromosome *11*, deficiencies, duplications, and inversions were constructed in embryonic stem cells with sizes ranging from 1 Mb to 22 cM. Two deficiencies and three duplications were established in the mouse germline. Mice with a 1-Mb duplication developed corneal hyperplasia and thymic tumors, while two different 3- to 4-cM deficiencies were embryonically lethal in heterozygous mice. A duplication corresponding to one of these two deficiencies was able to rescue its haplolethality.

ONE of the most common causes of human developmental disorders and fetal loss are chromosomal abnormalities such as inversions, duplications, deficiencies, translocations, and nondisjunction. Chromosomal changes that result in gene dosage differences (deletions, duplications, and nondisjunction) can be particularly severe. Chromosomal aberrations that cause minor perturbations in an embryonic cell's capacity to fulfill a developmental program may initially result in subtle developmental defects; however, these can be rapidly amplified by the developmental hierarchy, ultimately resulting in major developmental abnormalities. Consequently, many chromosomal alterations are incompatible with full-term fetal development. Some rearrangements are tolerated, however, and individuals may be born with a variety of clinical symptoms. For example, duplication of regions of chromosomes *21* and *17* cause Down syndrome (Epstein 1986) and Charcot-Marie-Tooth disease (Lupski *et al.* 1991), while DiGeorge syndrome has been shown to be associated with microdeletions of chromosome *22q11* (Driscoll 1994).

Alterations in chromosomes also occur spontaneously in somatic cells during the life of the organism, and these alterations are usually less of a problem to the organism. In many cases, somatic cells that suffer chromosomal damage that is deleterious to a cell may simply cause that cell to be lost from the organism and be replaced by cells from the same lineage with intact genomes. The genome of a differentiated somatic cell is not challenged with the rigor of executing an appropriate developmental program; therefore, somatic cells can usually tolerate genetic changes that would be very deleterious to an embryonic cell. Occasionally, however, an alteration may occur that allows a cell to obtain a specific growth advantage and to escape the normal mechanisms that might otherwise result in cell death. Such a cell may continue to proliferate and become neoplastic. Chromosomal alterations that cause ectopic expression of oncogenes (Rabbitts 1994) or loss of tumor suppressor genes (Marshall 1991; Weinberg 1991) are therefore selected in neoplasia.

Some chromosomal rearrangements, such as a simple translocation or an inversion, may affect just a few genes. For example, the inversions that disrupt the *X*-linked factor VIII gene cause severe hemophilia A (Lakich *et al.* 1993). The specific gene(s) associated with pathological deletions and duplications are, however, much harder to identify because many genes are affected by these aberrations. The generation of animal models that accurately recapitulate these types of genetic lesions will facilitate the study of human disease, and this will eventually enable the definition of specific gene-function relationships in these clinical syndromes.

Chromosomal rearrangements have been used extensively as an experimental tool in model organisms such as *Drosophila melanogaster*. Chromosomes with inversions (*Inv*; Sturtevant 1926) are used as balancers to maintain recessive mutations in specific linkage relationships by reducing recombination, while chromosome deficiencies (*Df*; Bridges 1917) and duplications (*Dp*; Bridges 1919) have been very useful for studying gene dosage and mapping genes in a defined genomic region. More importantly, chromosomal deficiencies are commonly exploited in genetic screens because a small portion of the genome is functionally hemizygous. Thus, the phenotype of a recessive mutation, which would normally be masked by the wild-type allele in the diploid context, will be readily detectable in the haploid state.

The similarity between humans and mice in many

Corresponding author: Allan Bradley, Department of Human and Molecular Genetics, Howard Hughes Medical Institute, Baylor College of Medicine, One Baylor Plaza, Houston, TX 77030.
E-mail: abradley@bcm.tmc.edu

salient aspects of mammalian anatomy and physiology, coupled with the close genome homology between these two species, makes mice an excellent model for illustrating the function of human genes. In many chromosome domains, the gene order is conserved between the two species (Watkins-Chow *et al.* 1996). The generation of mouse strains with defined chromosomal alterations will not only confirm the causative role of specific DNA rearrangements in human genetic diseases, but provide accurate models as well. Most chromosomal rearrangements described in the mouse have been induced by ionizing irradiation, and they are the outcome of studies initiated to examine the effects of radiation on the mammalian genome (Rinchik and Russell 1990). The deletions that arose in these studies are clustered around seven recessive and several dominant loci that result in readily identifiable phenotypes when deleted (Rinchik and Russell 1990). Although many of these existing deficiencies are poorly defined, they have proven to be invaluable for genetic studies of these particular regions. For example, the overlapping deletion series around the *albino* locus have been studied extensively to define the complementation groups that are implicated in early embryogenesis (Holdener-Kenny *et al.* 1992; Shumacher *et al.* 1996) and in saturated chemical mutagenesis screens (Rinchik 1991).

In the chromosome deficiencies induced by irradiation in mice, the induced breakpoints occur more or less randomly throughout the genome. Thus, the characterization of the size of a deficiency and identifying simple deficiencies from those that are associated with other rearrangements, such as translocations and inversions, can be labor intensive. Duplications can also be induced by X rays, although these are relatively rare events. This may be because this rearrangement is quite difficult to detect cytogenetically (especially when small), and also because the phenotypes of mice harboring DNA duplications can be subtle. Germline mutations are detected in X-irradiated mice at the rate of 1.5–3 $\times$ 10^{-4} per locus (Rinchik 1991). Thus, the generation of a specific set of DNA rearrangements by irradiation requires vast facilities that are available in very few laboratories. The chemical chlorambucil is an alternative to X irradiation for inducing deletions because this agent induces deletions at a much higher frequency of 1.3 $\times$ 10^{-3} per locus, although in mice it can also induce translocations (Rinchik *et al.* 1993).

Many germline modifications of single genes have been constructed by manipulating the genome in mouse embryonic stem (ES) cells (Bradley and Liu 1996). The largest deletion generated in the mouse by conventional gene targeting was 19 kb (Zhang *et al.* 1994). By combining homologous and *Cre-lox*P site-specific recombination, we have successfully generated a variety of chromosome rearrangements on the distal part of chromosome *11* in mouse ES cells (Ramirez-Solis *et al.* 1995) and established these altered chromosomes in mice. This portion of the mouse genome contains genes whose homologues map to human chromosome *17q*. All the rearrangements in this study are centered around the *Hsd17b1* locus, which is located close to the *Brca1* gene in the region that corresponds to human chromosome *17q21*. The intensive genetic studies involved in the search for the human *BRCA1* gene have yielded detailed genetic and physical maps of this region (Miki *et al.* 1995). In addition, several clinical cases have been reported that were associated with chromosomal deletions on *17q* (Park *et al.* 1992; Khalifa *et al.* 1993; Levin *et al.* 1995).

To begin to derive some functional information for this portion of the genome, a series of deficiencies, duplications, and inversions were generated and transmitted into the mouse germline, and the resulting phenotypes were examined. It was found that duplications of a 1.0-Mb region caused corneal hyperplasia and thymic tumors. Deficiencies of the two adjacent 6- to 8-Mb regions around the *Hsd17b1 (E_2DH)* locus caused early embryonic lethality in the heterozygous state, while the corresponding duplication of one region did not cause a detectable phenotype but was able to rescue the haplolethality of its deficiency counterpart.

MATERIALS AND METHODS

Genomic clones for gene targeting: Genomic clones for all the genetic loci in this study were isolated from a mouse 129/SvEv genomic library in lambda FIXII (Stratagene, La Jolla, CA). The hybridizations were routinely performed in 6$\times$ SSC, 0.1% nonfat dry milk at 65° overnight. Washes were usually performed in 1.0$\times$ SSC, 0.1% SDS at 65° for 20 min, and in 0.1$\times$ SSC, 0.1% SDS at 65° for 10 min, except for the human *Hsd17b1* probe, which was performed in 1.0$\times$ SSC, 0.1% SDS at 65° for 20 min.

Targeting the *Hprt*Δ3′ cassette to the *Hsd17b1* locus: The coding region of the mouse *Hsd17b1* gene (5.5 kb) was replaced by the *Hprt*Δ3′ cassette, which also contains the *Neo* gene and the 5′ half of truncated *Hprt* minigene (see Figure 2A), in both orientations (A or B). The 5′ diagnostic probe (PL16) hybridizes to a 15-kb *Eco*RI fragment from the wild-type allele. The fragments from the targeted alleles are 10.4 kb for A and 9.2 kb for B (Figure 1A). The targeted clones were confirmed with a 3′ diagnostic probe (PL17). Two targeted ES cell clones, A2.2L2E11 (orientation A, EA) and B2.2LB8 (orientation B, EB), were expanded, and their totipotency was tested by generating and breeding chimeras. Both cell lines produced germline-transmitting chimeras at a high frequency. They were used for further targeting as described below.

Targeting the *Hprt*Δ5′ cassette to the *Gas* locus: The 3.5-kb sequence containing the entire mouse *Gas*-coding sequence was replaced by the *Hprt*Δ5′ cassette, which contains puromycin-resistance gene (*Puro*) and the 3′ half of the truncated *Hprt* minigene (Figure 2A), in both orientations (GA or GB). The two targeting vectors were separately transfected into the EA and EB cell lines. Targeted clones were detected using the 5′ diagnostic probe (PG14), which detects a 12.5-kb *Pst*I wild-type fragment or a 10.2-kb (GA orientation) or a 8.5-kb *Pst*I (GB orientation) fragment from the targeted alleles

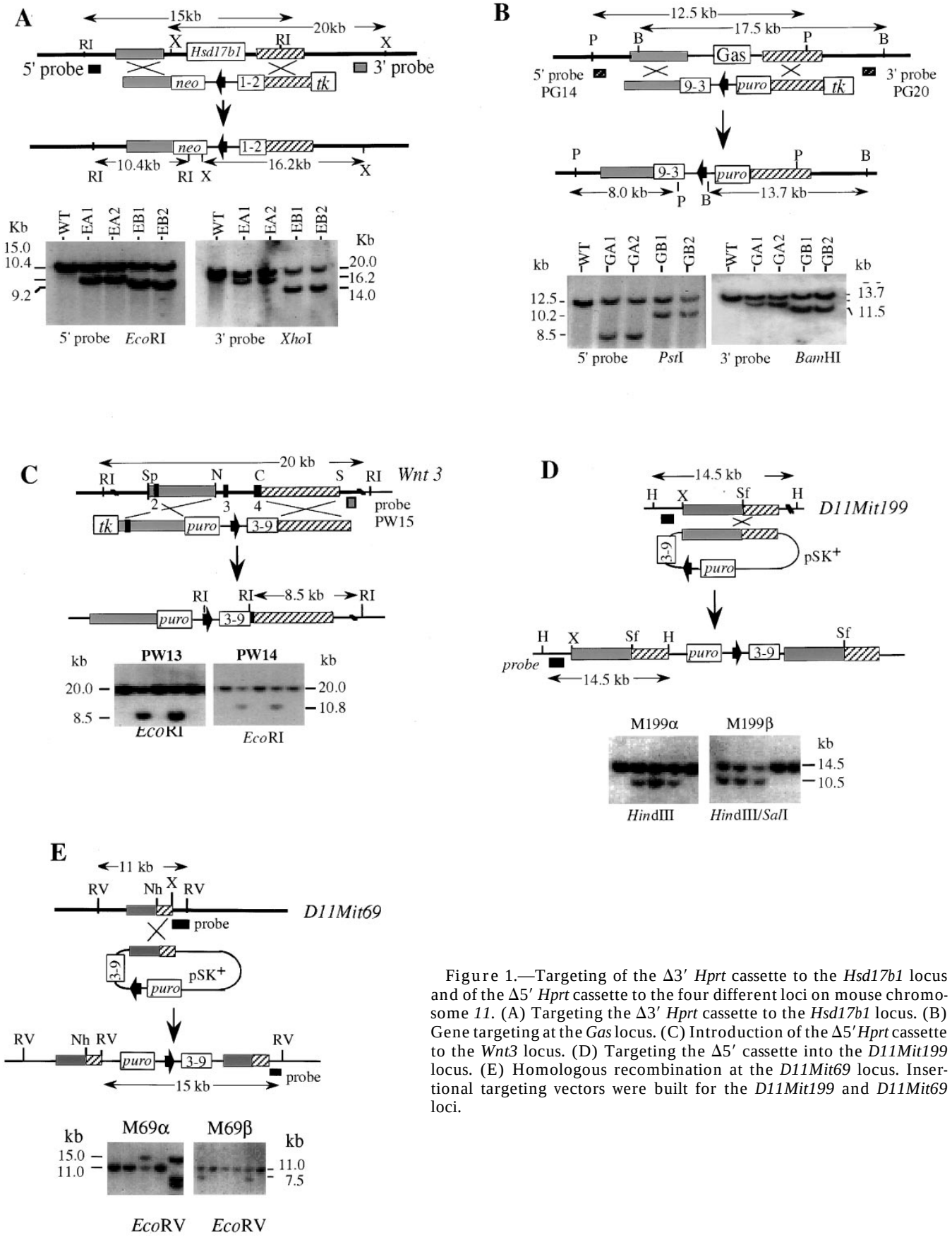

Figure 1.—Targeting of the Δ3′ *Hprt* cassette to the *Hsd17b1* locus and of the Δ5′ *Hprt* cassette to the four different loci on mouse chromosome *11*. (A) Targeting the Δ3′ *Hprt* cassette to the *Hsd17b1* locus. (B) Gene targeting at the *Gas* locus. (C) Introduction of the Δ5′*Hprt* cassette to the *Wnt3* locus. (D) Targeting the Δ5′ cassette into the *D11Mit199* locus. (E) Homologous recombination at the *D11Mit69* locus. Insertional targeting vectors were built for the *D11Mit199* and *D11Mit69* loci.

(Figure 1B). The targeted clones were further confirmed using the 3′ diagnostic probe (PG20).

Introducing the *Hprt*Δ5′ cassette to the *Wnt3* locus: Two replacement vectors (PW13 and PW14) that contain the *Hprt*Δ5′ cassette in both orientations replacing a 2.1-kb fragment (exon 3 and most of exon 4) of the *Wnt3* locus were built. This deletion will presumably create a null allele for the mouse *Wnt3* gene. The two targeting vectors were transfected into the EB cell line. DNA from the transfectants was digested with *Eco*RI and probed with a 0.75-kb fragment of PW15. The 20-kb wild-type fragment is altered to 8.5 or 10.8 kb in the PW13 and PW14 mutant alleles, respectively (Figure 1C).

Targeting the *Hprt*Δ5′ cassette to the *D11Mit199* and *D11Mit69* loci: *D11Mit199* and *D11Mit69* are anonymous microsatellite loci on mouse chromosome *11*. The *D11Mit199* locus is ~2 cM from the *Hsd17b1* locus and 1 cM from the *Wnt3*. The *D11Mit69* locus maps very close to the telomere of chromosome *11*, ~22 cM from the *Hsd17b1* locus. An arrayed mouse 129/SvEv genomic phage library was screened by PCR using primers specific for the *D11Mit199* locus (5′ATC GTC AAT AGG TGG CCA AG3′; 5′AGG AAA GGA TTC GGT ATC ATA GG 3′) and the *D11Mit69* locus (5′AGT TGC TGC AAT ATG GAC CC 3′; 5′ATC TCA GTG CTG TTC TAA CAC TGC3′). The genomic inserts of the positive phages were subcloned and used to construct the targeting vectors. In both cases, insertion vectors were constructed. An 8.0-kb *Not*I/*Xho*I fragment from the *D11Mit199* phage was used as the homology region for the two targeting vectors (m199α and m199β). These vectors were linearized with *Sfi*I (Figure 1D). Two insertion vectors were constructed from a 5.0-kb genomic fragment from the *D11Mit69* phage. *Nhe*I was used to linearize the vectors (m69α and m69β); one homology arm is 2.0 kb, and the other is 3.0 kb (Figure 1E).

ES cell culture and generation of chimeras: AB2.2 ES cells were used for gene targeting in this study. This cell line was derived from *Hprt*-deficient 129/SvEv mice (Matzuk *et al.* 1992). Embryonic stem cells were cultured and transfected according to described protocols (Ramirez-Solis *et al.* 1993). Typically, 20 μg linearized targeting vector DNA was electroporated into 1.0×10^7 ES cells that were subsequently selected with G418 (targeting the *Hsd17b1* locus), or in puromycin (targeting the *HoxB9*, *Gas*, *Wnt3*, *D11Mit199*, and *D11Mit69* loci), in the presence of FIAU (1-(2-dexyo-2-fluoro-*b*-D-arabinofuranosyl)-5-iodouracil). FIAU selection was omitted in the case of targeting the *D11Mit199* and *D11Mit69* loci. Clones were picked into 96-well arrays, and targeted ES cell clones were identified using Southern analysis (Ramirez-Solis *et al.* 1993). Transient expression of Cre was achieved by electroporating 20 μg of supercoiled pOG231 plasmid into 1.0×10^7 double-targeted ES cells. HAT (10 mm sodium hypoxanthine, 40 μm aminopterin, 1.6 mm thymidine) selection was initiated 24–48 hr after the electroporation.

Chimeras were generated by injecting ES cells into 3.5-day blastocysts from C57BL/6-c^{Brd}/c^{Brd} (a spontaneous albino mutant coisogenic C57BL/6 strain) females mated with C57BL/6-c^{Brd}/c^{Brd} males. The blastocysts were transplanted to the uterine horns of day-2.5 pseudopregnant foster mothers produced by mating F_1 (C57BL/6 × CBA) females with the vasectomized F_1 males (Bradley 1987). Chimeras were identified among the resulting progeny by their Black Agouti fur (ES cell-derived), and the male chimeras were subsequently bred to C57BL/6 or 129/SvEv females.

Southern analysis of genomic DNA: Genomic DNA was digested with restriction enzymes, run on a 0.7% agarose gel in 1.0× TAE buffer, and blotted onto a nylon membrane filter in 0.4 n NaOH overnight. The blot was neutralized in 2.0× SSC, 0.2 m Tris-HCl (pH 7.5) and baked at 80° for 30 min. The hybridization was performed in 1.5× SSC, 1.0% SDS, 0.5% fat-free milk, and 200 μg/ml denatured salmon testis DNA overnight at 65°. Washing was usually conducted in 1.0× SSC, 0.1% SDS at 65° for 20 min, and in 0.1× SSC, 0.1% SDS at 65° for 10 min. Probes were labeled with [α-^{32}P]dCTP using the QuickPrime kit from Pharmacia (Piscataway, NJ). For probes that contain repetitive sequences, preassociation of these probes with mouse genomic DNA was performed. In brief, purified labeled probes (25 ng in 100 μl) were mixed with 20–50 μg (50 μl) mouse genomic DNA and 100 μl hybridization solution. This probe mixture was heated at 100° for 5 min and then kept at 65° for 1–2 hr before it was added to a hybridization cylinder. Southern blots from such a hybridization were washed in regular stringency or washed at a higher temperature such as at 70°.

Fluorescent *in situ* hybridization: A mouse BAC library was screened by PCR using primers for *D11Mit199* for *D11Mit11*. Two positive BACs were identified: BAC 293C22 for the *D11Mit199* locus and BAC 330P14 for the *D11Mit11* locus (5′TAT TCT CTC CTT CCC CCC AC3′; 5′TAG AGT TGG GAC ACC CAA GC3′). BAC DNA was purified and used as probes for fluorescent *in situ* hybridization (FISH). Chromosome spreads from ES cells were prepared as described (Robertson 1987), with minor modification. FISH was performed according to the published protocol (Baldini and Lindsay 1994). BAC 330P14 was labeled with biotin and detected by FITC-avidin, which gave green fluorescence. The green color was converted to yellow color artificially for easy identification. BAC 293C22 was labeled with digoxigenin and detected by anti-digoxigenin-rhodamine, which gave red fluorescence.

PCR genotyping embryos: PCR was used to genotype embryos with the *Df11(2)* and *Dp11(2)* chromosomes. For detecting a chromosomal deficiency, primer 1 is from the human *Hprt* minigene exon 2, CCTCATGGACTAATTATGGAC; primer 2 is from the human *Hprt* minigene exon 9, CCAGTTT CACTAATGACACA. The product is 2.1 kb. To amplify the duplication allele, primer 1 was specific for the human *Hprt* minigene intron, 5′AGGATGTGATACGTGGAAGA3′, while primer 2 is specific to the *Pol*II promoter, 5′GCCGTTATTAG TGGAGAGGC3′. The PCR product is 770 bp.

Histological analysis: Embryos were processed for histological studies as described (Kaufman 1992). Briefly, the embryos were fixed in Bouin's solution overnight and then washed extensively in 70% ethanol until they were not yellow. After dehydration through a series of higher concentrations of ethanol, the embryos were embedded in paraffin wax. The embryos were sectioned at a thickness of 5–7 μm. Slides were stained with Hematoxylin (Harris) and counterstained with eosin. Similar histological procedures were used for analyzing eyes, spleens, thymuses, and tumors from the *Dp11(1)*/+ mice.

RESULTS

Generation of chromosomal deficiencies, inversions, and duplications: The strategy to generate the chromosomal rearrangements is illustrated in Figure 2. In brief, two complementary truncated *Hprt* minigene cassettes with an embedded *lox*P site were successively targeted to two loci on mouse chromosome *11* in ES cells (Figure 2A). Transient expression of Cre recombinase induces recombination between the two *lox*P sites, resulting in either a *Df*, a *Dp*, or an *Inv* (Figure 1C), depending on the relative orientation of the two cassettes. The recombination between the *lox*P sites reconstructs a full-length *Hprt* minigene from the complementary cassettes, enabling cell lines with these recombinant chro-

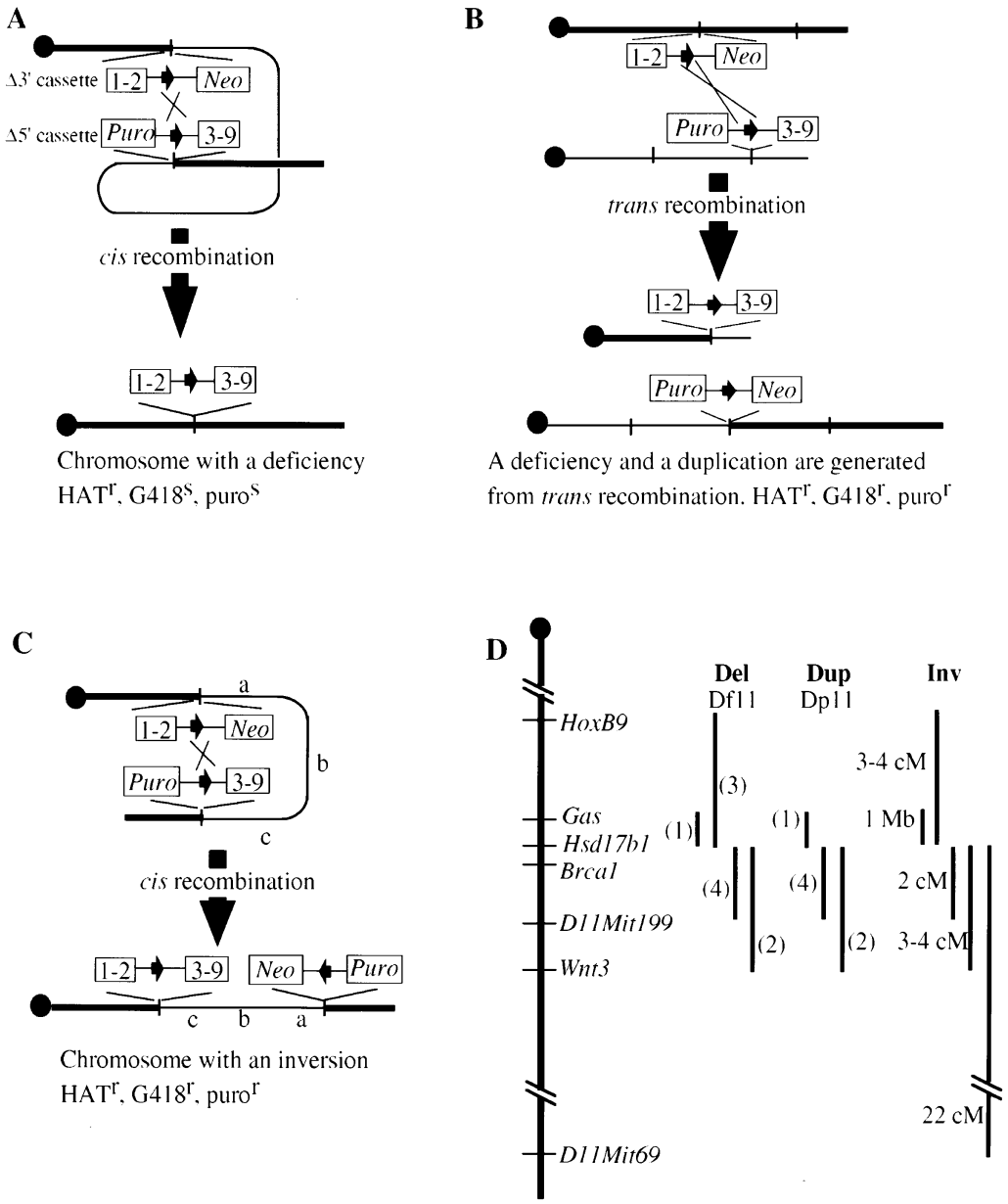

Figure 2.—(A) The strategy for generating chromosomal deletions (deficiencies). Two cassettes, *Hprt*Δ3′ and *Hprt*Δ5′, were targeted to two endpoints on a chromosome. Transient expression of Cre recombinase catalyzes the recombination and generates a deletion. (B) A deficiency and a duplication generated from *trans* recombination. (C) An inversion is expected if the Δ3′ and Δ5′ cassettes are in opposite orientation on a chromosome. (D) Summary of the chromosomal rearrangements on mouse chromosome *11*. Del (*Df11*), deficiency; Dup (*Dp11*), duplication; Inv, inversion.

mosomes to be directly selected in HAT. All the alterations described here have the *Hsd17b1* (*E_2DH*) locus as one of the endpoints. Therefore, this locus was targeted first with the *Hprt*Δ3′ vector in two different orientations (Figure 1A). The *Hprt*Δ5′ cassette was subsequently targeted to the loci around the *Hsd17b1* locus in these targeted cell lines. The targeting vectors and recombinant alleles generated with these vectors are summarized in Figure 1. The recombination endpoints included genes (*Gas*, *HoxB9*, and *Wnt3*) and microsatellite loci (*D11Mit199* and *D11Mit69*), and the targeting efficiencies were very similar for these loci (Table 1). Both replacement and insertion types of vectors were used (Figure 1). Targeting frequencies for these vectors were in the range of 5–20% of the double-resistant clones (G418 and FIAU, or Puro and FIAU) for the replacement vectors, and 20 and 8% of the puromycin-resistant clones for the *D11Mit199* and *D11Mit69* insertion vectors, respectively.

Double-targeted clones were transiently transfected with a supercoiled Cre expression plasmid, and HAT-resistant clones were isolated. The frequency of recombination varied, depending on the specific interval, the *cis* or *trans* configuration of the cassettes, and the type of rearrangement induced by the recombination event (Table 2). Recombination between the two cassettes when they have been targeted in direct orientation in *trans* will generate an ES cell with a *Df* on one chromosome and the corresponding *Dp* on the other. The frequency of *trans* recombination was generally much lower than recombination in *cis*, and the frequency of generating duplications (*cis*) was lower than the corresponding *Df* and *Inv* (Table 2). This may reflect the fact that *Dp cis* recombination can only be generated at the

TABLE 1

Targeting the two truncated *Hprt* cassettes into loci on mouse chromosome *11*

Genetic loci	*Hsd17b1*	*Gas*	*Wnt3*	*D11Mit199*	*D11Mit69*
Targeting frequency (%)[a]	5	5	15	20	8
Total homology length (kb)[b]	8.0	7.3	7	8	5
	4.3/3.7	3.6/3.7	3.0/4.0	3.0/5.0	3.0/2.0
Negative selection enrichment	3	3	5	N/A	N/A
Diagnostic enzyme	R	B	R	H3 for α	RV
				H3/S for β	
Probe for Southern[c]	2.1 kb	1.3 kb	0.75 kb	1.5 kb	2.5 kb
	N/RI	Rs	Hin/Xa	Nc/X	RV/X
	PL16	PG20	PW15	CMJ-7β	M69-7β

[a] The targeting efficiency of the same vector varied from one experiment to the next. For example, the *Hsd17b1* vectors had targeting frequencies in the range of 5–20%. The frequencies listed refer to the first experiment using a targeting vector. Two targeting vectors are built for each locus, which have similar targeting frequencies.

[b] The distribution of homology on the 5′ and 3′ sides of the targeting vectors. Insertion vectors were built for *D11Mit199* and *D11Mit69* loci.

[c] The plasmids from which the probes were derived are listed with the enzymes used for digestions. R, *Eco*RI; B, *Bam*HI; H3, *Hin*dIII; Hin, *Hin*cII; N, *Not*I; Nc, *Nco*I; Rs, *Rsa*I RV, *Eco*RV; S, *Sal*I; Xa, *Xba*I; X, *Xho*I. N/A, not applicable.

sister chromatid stage, while *Df* and *Inv* can also arise from recombination within a single chromatid. The abbreviations for the recombinant chromosomes are detailed in Table 3.

HAT-resistant clones were not recovered when the cassettes were in inverted orientation in *trans*. This is because the *trans* recombination frequency is very low, and acentric and dicentric chromosomes are the products from such a recombination event. Acentric chromosomes will be lost during cell division, and this will likely be a cell-lethal event because loss of this acentric fragment is equivalent to a homozygous deficiency, in this case covering 25% of chromosome *11*. If two inverted *lox*P sites are close to each other in *cis*, then two sister chromatids could theoretically recombine to form acentric and dicentric chromosomes at a high frequency, which would lead to loss of these cells. Although this has been observed in *D. melanogaster* (Golic 1994) and in mice (Lewandoski and Martin 1997), a marked decrease in the inversion frequency was not observed in the case of the smallest inversion described here (Table 2).

FISH analysis of chromosomal rearrangements: To characterize some of the chromosomal rearrangements in more detail, we performed FISH using probes from the *D11Mit199* and *D11Mit11* loci. Two BACs corresponding to these loci were isolated: 293C22 (*D11Mit199)* and 330P14 (*D11Mit11*). Figure 3 (A–D) shows the FISH analysis of wild-type control and a *Df11(2)/Dp11(2)* cell line that has a 3- to 4-cM deficiency and the same size duplication between the *Hsd17b1* and *Wnt3* loci. The FISH signals were artificially colored in red and yellow to distinguish the signals from the different BACs. In the case of the *Df11(2)/Dp11(2)* cell line, the deficiency chromosome domain can be identified in the interphase nucleus as a single red dot resulting from the *D11Mit11* BAC, which lies outside the deficiency, while the corresponding duplication chromosome has one

TABLE 2

Cre-*lox* recombination frequency on mouse chromosome *11*

	Deficiency		Inversion		Duplication	
Interval	*Cis*	*Trans*	*Cis*	*Trans*	*Cis*	*Trans*
Gas-Hsd17b1 (1 Mb)	476	1	355	0	166	2
Hsd17b1-D11Mit199 (2 cM)	102	3	293	0	NA	NA
HoxB-Hsd17b1 (3–4 cM)	2	0	43	0	NA	NA
Hsd17b1-Wnt3 (3–4 cM)	36	4	19	0	NA	NA
Hsd17b1-D11Mit69 (22 cM)	0	0	3	0	NA	NA

1.0×10^7 double-targeted ES cells were electroporated with 20 μg pOG 231 (cre expression plasmid) and selected with HAT medium. The numbers listed in the table refer to HAT^r colonies per electroporation, and they are the mean value of three to four independent cell lines. NA, not available.

red dot, but also two yellow dots, which is the signal from the *D11Mit199* BAC hybridization that is within the duplicated region. Because the duplicated region is relatively small, the duplicated signals could not be resolved as two discrete spots in a metaphase spread. However, the deficiency is clearly visible by the absence of a yellow spot corresponding to the *D11Mit199* locus.

We attempted to generate a 22-cM deficiency and the same size inversion between the *Hsd17b1* locus and the most distal microsattelite marker described for mouse chromosome *11*, *D11Mit69*. Six double-targeted clones for each orientation of the *D11Mit69* locus were generated and tested. Following cre transfection, a total of nine HAT-resistant clones were recovered from three double-targeted cell lines. Sib selection with puromycin and G418 indicated that these HAT-resistant clones had an inversion. This was confirmed by FISH analysis (Figure 3, A and E). Both probes (*D11Mit199* and

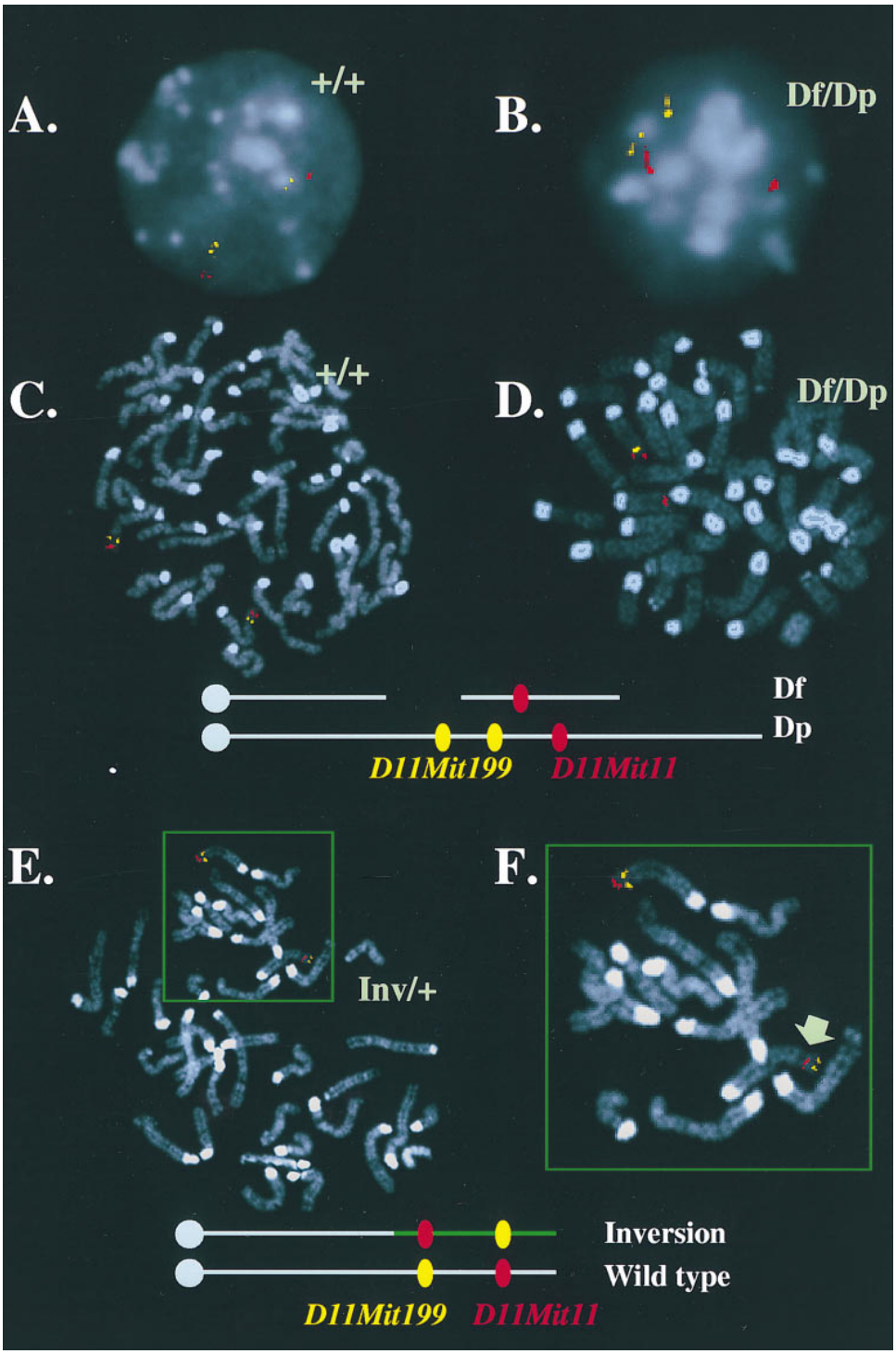

Figure 3.—FISH analysis of the chromosomal rearrangements. The two BAC probes used in this study were isolated using primers from the *D11Mit199* and *D11Mit11* loci. The *D11Mit199* BAC is shown as yellow and the *D11Mit11* locus is colored red. These loci are ~10 cM apart on mouse chromosome *11* (Dietrich *et al.* 1996). (A and C) Interphase nuclei and metaphase chromosome preparations of wild-type ES cells, respectively. (B and D) Interphase nuclei and metaphase chromosome preparations, respectively, from the A-PW13-A6 (#2 clone), which was confirmed to possess a 3–4-cM deficiency [*Df11(2)*], and the corresponding duplication [*Dp11(2)*] between the *Hsd17b1* and *Wnt-3* loci. (E) The metaphase spread that has a 22-cM inversion between the *Hsd17b1* and *D11Mit69* loci. Both probes (*D11Mit199* and *D11Mit11*) are within this inverted segment. (F) The enlarged view of the wild-type chromosome *11* and the chromosome *11* with the 22-cM inversion (arrowed). Diagrams below the FISH images illustrate the interpretation of the hybridization signals. The green area represents the inverted region on chromosome *11*.

TABLE 3

Chromosome abbreviations

Chromosome	Size (Mb)	Abbreviation
del(*11*)(gas-Hsd17b1)^{Brd}	1	*Df11(1)*
del(*11*)(Hsd17b1-Wnt3)^{Brd}	6–8	*Df11(2)*
del(*11*)(Hoxb9-Hsd17b1)^{Brd}	6–8	*Df11(3)*
del(*11*)(Hsd17b1-D11Mit199)^{Brd}	3–4	*Df11(4)*
dp(*11*)(gas-Hsd17b1)^{Brd}	1	*Dp11(1)*
dp(*11*)(Hsd17b1-Wnt3)^{Brd}	6–8	*Dp11(2)*
dp(*11*)(Hsd17b1-D11Mit199)^{Brd}	3–4	*Dp11(4)*

D11Mit11) lie within the inverted region, and metaphase analysis clearly shows that the order of these probes with respect to the centromere has been reversed in the inversion chromosome. HAT-resistant recombinants were not recovered from the other three double-targeted clones with the same orientation of the *Hprt*Δ*5′* cassette, indicating the two cassettes are likely to be in *trans* in these cell lines.

None of the six cell lines with the *Hprt*Δ*5′* cassette in the opposite orientation gave HAT-resistant clones. There are two possible explanations: either all of these were targeted in the *trans* configuration and the recombination frequency is below the threshold of detection, or the 22-cM deficiency induced by the *cis* recombination causes cell lethality in the heterozygote state.

***Dp11(1)* causes corneal hyperplasia and thymic neoplasia:** Using *Df11(1)*/*Dp11(1)* genetically balanced ES cells, chimeric mice were generated, and the Df and Dp chromosomes were segregated during germ line transmission, allowing them to be analyzed independently. Both *Dp11(1)*/+ and *Df11(1)*/+ mice were obtained and initially appeared overtly normal. However, the two genotypes were present at a 2:1 ratio (*Dp:Df*), rather than at the expected 1:1 ratio, when mice were genotyped at 3 wk of age (Table 4), but this ratio distortion was not observed in subsequent generations.

The *Dp11(1)*/+ and *Df11(1)*/+ mice initially appeared to be unremarkable and had normal fertility. As the *Dp11(1)*/+ animals aged, however, their eyes became opaque. Histological analysis of the eyes showed that this was caused by corneal hyperplasia (Figure 4, A–C). The early changes in the corneal lesions consisted of epithelial hyperplasia and increased vascularity. More advanced lesions showed small aggregates of polymorphonuclear leukocytes, marked polypoid subepithelial and epithelial thickening, and ulceration. Intercrossing *Dp11(1)*/+ mice resulted in the generation of *Dp11(1)*/*Dp11(1)* homozygotes. These were recovered at the expected 25% frequency and appeared to be initially normal, though both males and females had reduced fertility. Like the *Dp11(1)*/+ heterozygous mice, these animals exhibited the same corneal defect, but with a shorter latency (Figure 4D). The *Dp11(1)*/*Dp11(1)* homozygotes and *Dp11(1)*/+ mice also developed thymic tumors. By 10 mo of age, ~20% of these mice (heterozygotes and homozygotes, $n = 22$) had these tumors. These tumors were characterized by massive enlargement of the thymus, and they showed enlarged nuclei with prominent nucleoli with an increased mitotic activity. Grossly enlarged spleens were also noted in some animals, and many of these exhibited lymphoid and myeloid hyperplasia (Figure 5). Some were accompanied by chronic inflammation of undetermined etiology in the liver and other organs.

Taken together, these data strongly suggest that there exists a dosage-sensitive gene (or genes) within this 1000-kb interval. Relatively modest increases in gene dosage (50%) in the case of the *Dp11(1)*/+ heterozygotes were sufficient to confer corneal hyperplasia and predisposition to thymic neoplasia.

The *Df11(2)* chromosome is haplo-insufficient during early embryogenesis: Chimeras were generated from *Df11(2)*/*Dp11(2)* ES cells produced from the *trans* recombination event. Test breeding of these chimeras resulted in repeated transmission of the *Dp11(2)* chromosome ($n = 33$), but the corresponding *Df11(2)* chromosome was never recovered. It was therefore evident that the *Df11(2)* chromosome caused embryonic lethality in the heterozygotes.

While there are several possible explanations for this, such as imprinting or position effects, the most likely explanation is haploinsufficiency caused by the loss of specific genes. To distinguish between these hypotheses, *Dp11(2)*/+ females were backcrossed to the *Df11(2)*/*Dp11(2)* chimeric males. Mice that had the *Df11(2)* chromosome, but only in combination with the *Dp11(2)* chromosome, were recovered from these matings. These

TABLE 4

Germline transmission of engineered chromosomes from chimeras

Interval	ES cells[a]	Genetic distance	Deficiency	Duplication	Wild type	DT
Hsd17b1-Gas	*Df/Dp*	1000 kb	27	48	NA	NA
Hsd17b1-HoxB	*Df/+*	3–4 cM	0	NA	31	1
Hsd17b1-Wnt3	*Df/Dp*	3–4 cM	0	33	NA	NA

[a] Most chimeric mice were derived from ES cells that are genetically balanced: a deficiency on one chromosome *11* and a duplication counterpart on the other chromosome *11*. These two chromosomes are segregated in meiosis. Therefore, both *Df/+* and *Dp/+* are expected from such chimeras. DT, mice have a chromosome with the two truncated *Hprt* cassettes; NA, not applicable.

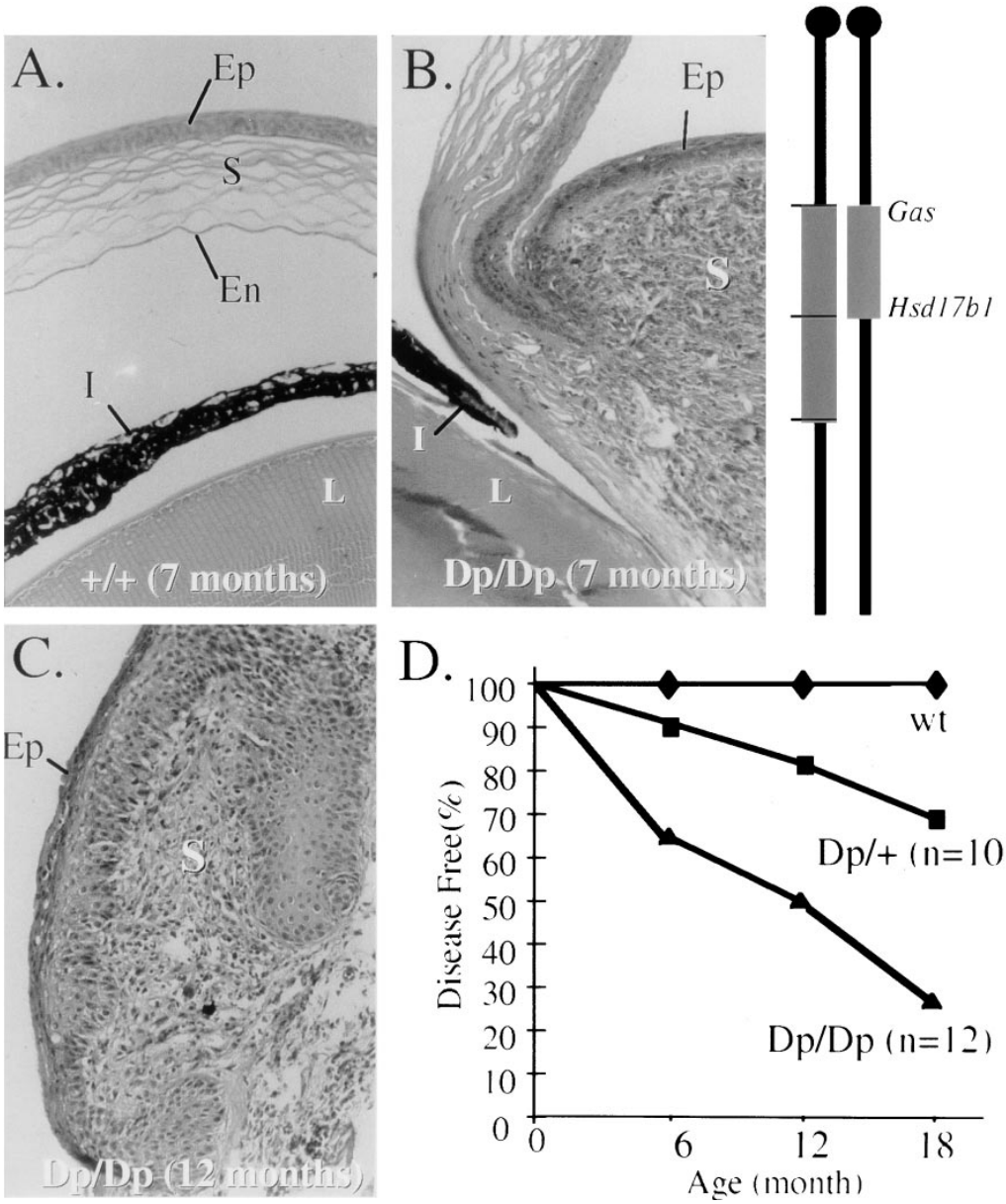

Figure 4.—Histological studies of the eyes of *Dp11(1)*/+ and *Dp11(1)*/*Dp11(1)* mice. (A) Section of the eye of a wild-type mouse (7 mo). (B) Section of the eye of a *Dp11(1)*/*Dp11(1)* mouse (7 mo). (C) Section of the cornea of a *Dp11(1)*/*Dp11(1)* mouse (12 mo). (D) The incidence of corneal hyperplasia is correlated with gene dosage. Ep, corneal epithelium; En, corneal endothelium; S, stroma; L, lens; I, iris.

Dp11(2)/*Df11(2)* mice are overtly normal and fertile, allowing the *Df11(2)* chromosome to be maintained by intercrossing *Df11(2)*/*Dp11(2)* mice. From these crosses, 30/46 (67%) of the mice were *Df11(2)*/*Dp11(2)* compound heterozygotes, while 16/46 (33%) are homozygous for the *Dp11(2)* chromosome. These are the expected ratios because the *Df11(2)* is highly unlikely to be viable in the homozygous state, given that this 3–4-cM interval will contain an estimated 200–300 genes. The loss of the *Df11(2)* heterozygotes and homozygotes occurs before birth because the average litter size in these crosses is reduced to 4.4 from 8 for wild-type matings. The *Dp11(2)*/+ and *Dp11(2)*/*Dp11(2)* mice are fertile and normal at the age of 1 yr.

To characterize the basis of the *Df11(2)*/+ embryonic lethality, timed matings were established between *Df*/*Dp* males and wild-type females so that half of the conceptuses would be *Df11(2)*/+. The resulting embryos were dissected from the decidua, and the yolk sac DNA was genotyped by PCR. Approximately half of the conceptuses recovered at E8.5 and E7.5 were abnormal, or the embryos were in the process of resorption. These abnormal embryos were much smaller at E7.5 days than the normal E7.5 embryos, and they overtly resembled E6.5 embryos. All the abnormal embryos (n = 36) had inherited the *Df11(2)* allele, while the morphologically normal embryos were *Dp11(2)*/+ heterozygotes. At 9.5 days, all the abnormal conceptuses were totally resorbed and could not be genotyped.

To further investigate the embryonic lethality, *Df11(2)*/+ embryos were examined histologically. Embryos were collected at E5.5 (n = 10), E6.5 (n = 20), and E7.5 (n = 22), processed, and transversely and sagittally serially sectioned. At E5.5, there was no obvious difference between the *Df11(2)*/+ embryos and their *Dp11(2)*/+ littermates. Coincident with the onset of

gastrulation at E6.5, approximately half of the embryos could be distinguished from their *Dp11(2)*/+ littermates. Overall, these abnormal embryos were much smaller, there was no clear demarcation between the embryonic and extra-embryonic portions, and the embryonic ectoderm cells were packed loosely and lacked the typical elongated shape seen in the normal embryos (Figure 6, A and B).

By E7.5, wild-type embryos have progressed through gastrulation, there is extensive mesoderm present, and the embryos have formed the chorion, amnion, and visceral yolk sac. At the same gestational stage, the *Df11(2)*/+ embryos do not appear to have progressed much beyond 6.5 days of development (Figure 6, C and D). While the visceral endoderm appears to be overtly normal in the *Df11(2)*/+ embryos, there is no evidence of mesoderm formation, and the embryonic and extra-embryonic ectoderm layers appear to be markedly deficient. In particular, the embryonic ectoderm cells were restricted to the distal end of the embryos and were dying. In mice, gastrulation coincides with a period of exceedingly rapid cell proliferation as the embryo accumulates the minimum threshold number of 1400–1500 epiblast cells required to initiate gastrulation (Power and Tam 1993). It is possible that the *Df11(2)*/+ epiblast cells have a reduced rate of proliferation compared to *Dp11(2)*/+ epiblast cells at this critical developmental stage, and, therefore, *Df11(2)*/+ embryos do not accumulate the required number of epiblast cells for gastrulation.

To examine the possibility of a reduced cell cycle rate, we determined the mean cell cycle rate of *Df11(2)*/+ ES cells. A mean doubling time of 24 hr was measured, which is indistinguishable from that of the wild-type ES cells. To investigate the possible developmental specificity of this defect, *Df11(2)*/+ ES cells were used to generate chimeras by blastocyst injection into wild-type embryos. These chimeras had extensive contributions from the injected ES cells. This indicates that cells with this large deficiency are viable as terminally differentiated somatic cells when rescued through early embryogenesis by wild-type cells.

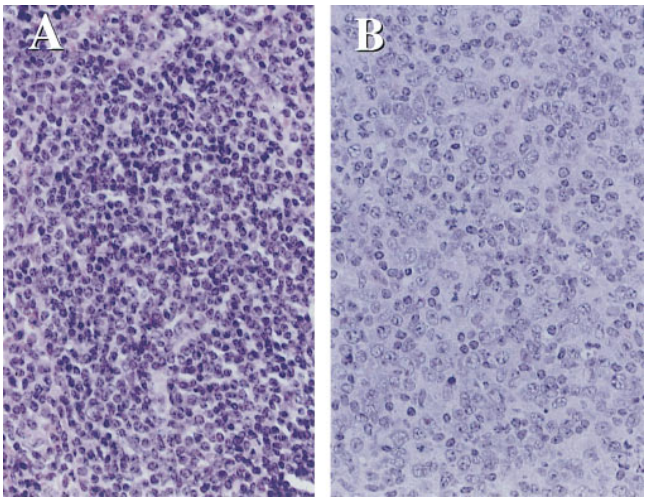

Figure 5.—Histopathological analysis of the lymphomas in mice with the 1-Mb DNA duplication. (A) Wild-type spleen. Note the benign cytological features in lymphocytes comprising the white pulp. (B) Malignant lymphoma of the thymus, exhibiting nuclear enlargement, prominent nucleoli, and frequent mitotic figures. ×128.

***Df11(3)* causes haplolethality:** *Df11(3)*/+ ES cells were used to generate chimeras. Out of 32 germline transmission pups, 31 inherited the wild-type chromosome *11*, while 1 had the double-targeted chromosome *11* where the *Hprt*Δ3′ and *Hprt*Δ5′ cassettes are at the *Hsd17b1* and *HoxB9* loci, respectively (presumably derived from minor contamination of the parental double-targeted ES cells in the HAT^r clones with the deficiency as the result of cross-feeding among $Hprt^-$ and $Hprt^+$ cells). The fact that the mice with the deficiency were not recovered indicated that the *Df11(3)* also leads to haplolethality. The availability of mice with the double-targeted chromosome *11* will make it possible to establish *Df11(3)* in somatic cells. The Cre-lox recombination efficiency for generating the *Df11(3)* was very low compared to that of *Df11(2)*; consequently, to date, it has not been possible to derive the balanced *trans*-recombination product *Df11(3)*/*Dp11(3)* and study this haploinsufficiency further.

DISCUSSION

Large DNA rearrangements and their frequency: With the development of high-resolution genetic maps of the mouse genome including >6500 microsatellite markers (Dietrich *et al.* 1996), specific chromosome alterations can be rapidly constructed for a specific purpose with the *Hprt-loxP-Cre* selectable system used in this study. In many cases, the relative position of the two loci on a chromosome will be known from genetic maps. These genetic loci can be readily prepared as recombination endpoints using conventional targeting vectors. To generate a full repertoire of rearrangements, it is necessary to target one cassette to an anchor point, in both orientations. In most cases, the relative orientations of the loci selected for endpoints will not be known, but they can be inferred by determining which of the four possible configurations of the cassettes is able to produce the deficiency. This is not difficult to determine because the neomycin- and puromycin-selectable markers are lost only when deficiencies are generated from recombination events where the cassettes have been targeted in *cis*. Once the relative orientations are determined for a pair of markers, this information can be used in the design of subsequent experiments in which only two possible combinations may need to be tested.

If a deficiency is generated by recombination on the same chromatid or chromosome, then the reciprocal recombination product is a ring chromosome that will

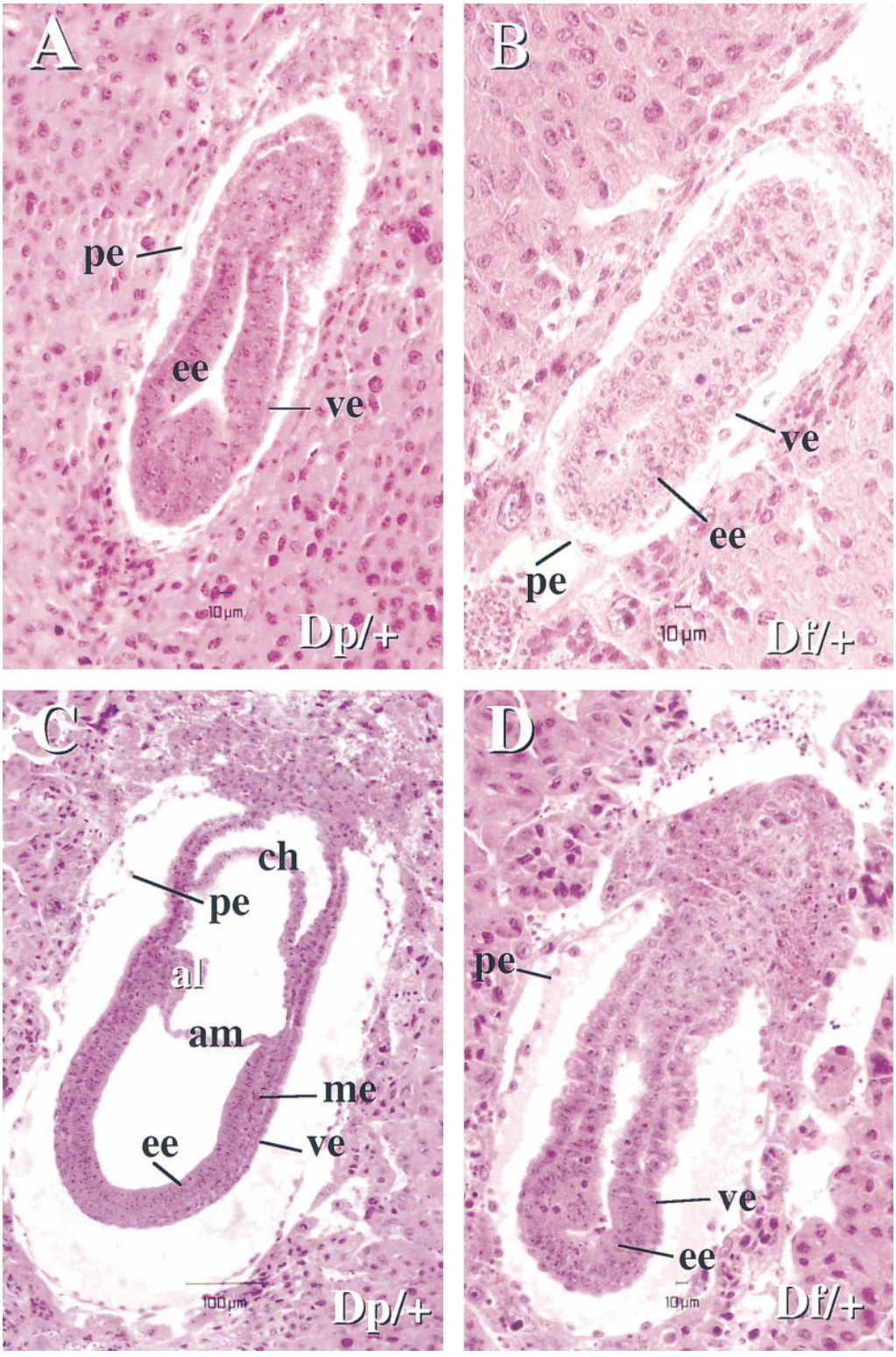

Figure 6.—Histological analysis of embryos with the 3–4-cM deficiency and the duplication. (A) E6.5 day embryo of *Dp11(2)*/+. (B) E6.5 day embryo of *Df11(2)*/+. (C) E7.5 day embryo of *Dp11(2)*/+. (D) E7.5 day embryo of *Df11(2)*/+. am, amnion; ch, chorion; ee, embryonic ectoderm; me, mesoderm; pe, parietal endoderm; ve, visceral endoderm; al, allantois.

be lost in subsequent cell divisions. Such molecules have been detected as FLP-FRT recombination products in nondividing cells in *D. melanogaster* (Ahmad and Golic 1996). We have not been able to detect ring molecules in ES cells, presumably because these products are rapidly lost in the process of normal cell growth.

Recombination between *lox*P sites with the same orientation in *trans* can generate ES cells with a deficiency accompanied by a duplication, regardless of the relative orientation of the two cassettes along a chromosome. The recombinant chromosomes will differ slightly, depending on the relative order of the *Hprt* cassettes. In one case, the chromosome with the deficiency will be tagged with the regenerated *Hprt* minigene, while the

chromosome with the duplication will carry the neomycin- and puromycin-resistance cassettes. If the two cassettes are oppositely oriented, then the chromosome with the deficiency will carry the neomycin- and puromycin-resistance genes, and the chromosome with the duplication will carry the *Hprt* minigene.

The recombination frequency between *lox*P sites on the same chromosome appears to decrease as the distance between the *lox*P sites increases (Table 2). Similar observations have been reported in experiments in *D. melanogaster* using the FLP-FRT system (Golic and Golic 1996). It is possible that this distance factor could reflect limiting time of availability and/or concentration of Cre caused by the transient expression system used in our experiments, and that this distance frequency relationship may vary under conditions of constitutive Cre expression.

The frequency of recombination between *lox*P sites in *trans* is always 10^{-2}- to 10^{-3}-fold lower than the equivalent recombination event when the *lox*P sites are on the same chromosome. However, the frequency of recombination in *trans* does not exhibit significant distance dependence, at least over the 1 Mb to 3- to 4-cM intervals tested in this study. The fact that we were unable to recover translocations using the cassettes used in this study (data not shown) suggests that recombination between homologous chromosomes is more frequent than that between two nonhomologous chromosomes. This also suggests that interactions between nonhomologous chromosomes occur less frequently than those between the homologues.

In this study, we have examined recombination between *lox*P sites positioned 3–4 cM apart in two adjacent regions (*HoxB-Hsd17b1* and *Hsd17b1-Wnt3*) on chromosome *11*. Despite the similar size of these intervals, they yielded very different recombination frequencies (Table 2). The *cis* recombination frequency between the *HoxB* and *Hsd17b1* loci is similar to the frequency of *trans* recombination between the *Hsd17b1* and *Wnt3* loci. Other recombination events in the *HoxB* cluster have also been quite low; *e.g.*, the frequency of deleting a 90-kb fragment in the *HoxB* cluster was lower than obtaining a 1.0-Mb deficiency between the *Gas* and *Hsd17b1* loci (Ramirez-Solis *et al.* 1995). These data indicate that the efficiency of this system is position dependent. This might be caused by target accessibility of Cre recombinase (Sauer and Henderson 1988) or might reflect the physical proximity of various chromosomal domains.

It was not possible to obtain ES cells with a heterozygous 22-cM *Df* between the *Hsd17b1* and *D11Mit69* loci; however, clones with the corresponding inversion could be obtained, confirming that Cre could mediate recombination over this large distance. It is therefore likely that this specific deficiency results in slow growth or cell lethality in ES cells as a consequence of either the loss of a single highly dosage-sensitive gene or the cumulative effect of the simultaneous loss of one copy of many slightly dosage-sensitive genes. Although clones with the combination *Df*/*Dp* status over this 22-cM interval should have been recovered, the failure to recover such clones indicates that the *trans* recombination frequency is quite low in this instance. It is interesting to note that this region of the genome is frequently deleted in both human and mouse tumors, indicating that the survival/proliferation phenotype observed in ES cells may be specific to this cell type because these ES cells can develop into certain somatic cell types in chimeric mice, and cells with a corresponding deficiency have the ability to proliferate as tumor cells. Similar differences have been observed in some other genes; *e.g.*, both *Brca1* (Hakem *et al.* 1996) and *Brca2* (Sharan *et al.* 1997) are essential for survival in ES cells, but tumor cells deficient in these gene products are able to proliferate.

Gene dosage effects: Gene dosage plays an important role in diseases in humans and mice. There are several genes that are known to exhibit striking dosage effects. For example, heterozygous mutations in *Pax6* cause the *small eye* phenotype in mice (Hill *et al.* 1991) and Aniridia in humans (Gessler *et al.* 1989). Similarly, mutations in *Pax3* cause white belly spots in mice (Epstein *et al.* 1991) and Waardenburg syndrome in humans (Tassabehji *et al.* 1992). There are other regions of the human genome that exhibit gene dosage effects resulting from an increased as well as decreased gene dosage (Fisher and Scambler 1994). Several clinical syndromes are caused by gene dosage alterations on human chromosome *17*; *e.g.*, Charcot-Marie-Tooth type 1A is caused by a 1.5-Mb duplication in *17q12* (Lupski *et al.* 1991), while deficiency of the same region leads to hereditary neuropathy with liability to pressure palsies (Chance *et al.* 1993). The Smith-Magenis syndrome has recently been found to have an ~10-Mb DNA deletion in *17p11.2* (Chen *et al.* 1997).

Of the hundreds of published knockouts in the mouse, only one has been reported to exhibit an embryonic haplolethality phenotype (Ferrara *et al.* 1996). Although these genes only represent a small sample of the entire mouse genome, these results indicate that the number of haplolethal genes is likely to be quite low in the mouse. It has been estimated that only three or four loci are truly haplolethal in *D. melanogaster*, the other model organism that has been most extensively studied in the context of chromosomal variants (Lindsley *et al.* 1972). Similarly, the presence of haplolethality can be examined in mice carrying large DNA deficiencies. Viable mice have been generated with deletions using ionizing irradiation, and these deficiencies collectively have been estimated to cover ~8% of the mouse genome (defined cytogenetically) in one study (Cattanach *et al.* 1993). In some cases, these deficiencies are very large, and mice carrying deletions covering 30% of chromosome *14* or 22% of chromosome *1* were reported to be viable (Cattanach *et al.* 1993). However, the deletions generated by irradiation of mice have been biologically selected to be viable and cytogenetically visi-

ble. This selection criterium is likely to favor regions of the genome with a low gene density. Furthermore, without a duplication counterpart chromosome present, the haplolethality can be difficult to detect. In this study, both the *Hsd17b1-Wnt3* [*Df11(2)*] and the *Hsd17b1-HoxB* [*Df11(3)*] deficiencies led to lethality in the heterozygous state; this was not caused by heterozygous deficiency for the anchor loci because these have been evaluated independently and do not exhibit any phenotype. We have demonstrated that the haplolethality of the *Df(2)* was caused by alteration of gene dosage. At this time, we cannot discriminate if this lethality is caused by a single gene or by many genes that map over this region. It has been demonstrated that the gene density in the region of human chromosome *17* that corresponds to this region of mouse chromosome *11* is unusually high (Schuler *et al.* 1996). Specific subdeletions can be generated rapidly with our chromosome engineering system. Cell lines carrying both a duplication and a deficiency within the *Df11(2)* interval have been generated between the *Hsd17b1* and *D11Mit199* loci [*Df11(4)*/*Dp11(4)*]. Transmission of these chromosomes into the mouse genome will enable us to generate *Df11(2)*/*Dp11(4)* and *Df11(4)*/+ mice. These mice will facilitate a refinement of the haplolethality critical region and enable the identification of the gene(s) involved.

Dp11(1)/+ and *Dp11(1)*/*Dp11(1)* mice have various abnormalities, while the *Dp11(2)*/+ and *Dp11(2)*/*Dp11(2)* mice do not exhibit any phenotype. This confirms that the phenotypes seen in the *Dp11(1)*/+ mice are most likely caused by specific genes in this 1.0-Mb interval. The most penetrant of these is the corneal hyperplasia, which occurs in 80% of the *Dp11(1)*/*Dp11(1)* mice. Interestingly, the latency and penetrance of the eye phenotype is dosage dependent. The development of lymphoma also indicates that there exists a highly dosage sensitive gene(s) within this 1.0-Mb interval. It is not possible to determine if the eye and thymic tumor phenotypes are the consequence of an increased dosage of the same or different genes. Because this interval is relatively small, mouse BAC contigs are being assembled to span this region. The phenotypes associated with individual BAC clones will be assessed in transgenic mice. This will help to separate the phenotypes associated with the duplication of this region to different BACs, and these clones eventually can be used to identify the gene(s) that are causing these phenotypes.

With the increasing resolution of the regions of conservation between the mouse and human genomes, as well as a more detailed understanding of chromosomal diseases in the human genome, it is evident that similar deficiencies, duplications, and other chromosomal rearrangements can be recapitulated in the mouse. The construction of subrearrangements will also enable the identification of the genes responsible for specific phenotypes in patients. Equally important is that mice heterozygous for a deficiency are functionally hemizygous for this chromosomal region. This will be a very valuable resource for saturated genetic screens with a set of deficiencies covering the entire mouse genome. The power of such screens has been demonstrated in Drosophila (Ashburner 1989) and in the existing deficiency collections in mice (Rinchik 1991).

An alternative method for generating chromosomal deficiencies in the mouse has been reported recently (You *et al.* 1997; Thomas *et al.* 1998). In this system, a negative selectable marker is targeted to the region of interest in a hybrid ES cell line, the cells are irradiated, and clones that have lost the negative selectable cassette can be selected. Although many chromosomal deletions can be rapidly generated using this approach, the breakpoints are randomly distributed and, therefore, require detailed characterization with respect to their size and the exclusion of complex rearrangements. In addition, the definition of the endpoints can be particularly time consuming. The detection of chromosome deficiencies generated by this method also depends on the density of polymorphic markers in the region of interest. The clustering of polymorphisms between certain strains may limit the application of this method to generate nested series of deletions to specific regions of the genome. Moreover, deficiencies in haplolethality regions, inversions, and duplications are unlikely to be recovered by this selection procedure. The Cre-*lox*P system described here obviates many of these problems.

In summary, a series of large DNA rearrangements have been generated in ES cells and established in the mouse germline. Analysis of mice with these engineered chromosomes has identified a 1000-kb region that contains a gene(s) which causes tumorigenesis when overexpressed. A contiguous 12- to 16-cM region of the genome is dosage sensitive (*HoxB-Wnt3*), resulting in early embryonic lethality in the heterozygotes. Further studies will allow the isolation of genes responsible for these phenotypes. The data described here demonstrate that precise manipulation of chromosome segments in mice is possible. This will not only facilitate the modeling of various human "chromosomal diseases," but it will also provide rich resources for functional genomic studies in the mouse.

We thank Dr. Antonio Baldini and Vesna Jurecic for assistance in FISH analysis; Eva Regal for blastocyst injection; Dr. Weiwen Cai for providing the two BACs for FISH analysis; Dr. Guangbin Luo, Dr. Alea Mills and Binhai Zheng for comments on this manuscript. This work was supported by grants from the National Institutes of Health. P.L. has been supported by a predoctoral fellowship from the Markey Foundation. A.B. is an investigator with the Howard Hughes Medical Institute.

LITERATURE CITED

Ahmad, K., and K. G. Golic, 1996 Somatic reversion of chromosomal position effects in *Drosophila melanogaster*. Genetics **144:** 657–670.

Ashburner, M., 1989 *Drosophila: A Laboratory Manual*. Cold Spring Harbor Laboratory Press, Cold Spring Harbor, NY.

Baldini, A., and E. Lindsay, 1994 Mapping human YAC clones by fluorescence in situ hybridization using Alu-PCR from single yeast colonies, pp. 75–84 in *In Situ Hybridization Protocols*, edited by K. H. A. Choo. Humana Press, Totowa, NJ.

Bradley, A., 1987 Production and analysis of chimeric mice, pp. 113–151 in *Teratocarcinomas and Embryonic Stem Cells - A Practical Approach*, edited by E. J. Robertson. IRL, Oxford.

Bradley, A., and P. Liu, 1996 Target practice in transgenics. Nat. Genet. **14:** 121–123.

Bridges, C. B., 1917 Deficiency. Genetics **2:** 445–465.

Bridges, C. B., 1919 Duplications. Anat. Rec. **15:** 357–358.

Cattanach, B. M., M. D. Burtenshaw, C. Rasberry and E. P. Evans, 1993 Large deletions and other gross forms of chromosome imbalance compatible with viability and fertility in the mouse. Nat. Genet. **3:** 56–61.

Chance, P. F., M. K. Alderson, K. A. Leppig, M. W. Lensch, N. Matsunami *et al.*, 1993 DNA deletion associated with hereditary neuropathy with liability to pressure palsies. Cell **72:** 143–151.

Chen, K.-S., P. Manian, T. Koeuth, L. Potocki, Q. Zhao *et al.*, 1997 Homologous recombination of a flanking repeat gene cluster is a mechanism for a common contiguous gene deletion syndrome. Nat. Genet. **17:** 154–163.

Dietrich, W. F., J. Miller, R. Steen, M. A. Merchant, D. Damron-Boles *et al.*, 1996 A comprehensive genetic map of the mouse genome. Nature **380:** 149–152.

Driscoll, D. A., 1994 Genetic basis of DiGeorge and velocardiofacial syndromes. Curr. Opin. Pediatr. **6:** 702–706.

Epstein, C. J., 1986 *The Consequences of Chromosome Imbalance: Principles, Mechanism and Models*. Cambridge University Press, Cambridge, UK.

Epstein, D. J., M. Vekemans and P. Gros, 1991 *splotch* (*Sp*^{2H}), a mutation affecting development of the mouse neural tube, shows a deletion within the paired homeodomain of *Pax-3*. Cell **67:** 767–774.

Ferrara, N., K. Carver-Moore, H. Chen, M. Dowd, L. Lu *et al.*, 1996 Heterozygous embryonic lethality induced by targeted inactivation of the VEGF gene. Nature **380:** 439–442.

Fisher, E., and P. Scambler, 1994 Human haploinsufficiency—one for sorrow, two for joy. Nat. Genet. **7:** 5–7.

Gessler, M., K. O. Simola and G. A. Bruns, 1989 Cloning of breakpoints of a chromosome translocation identifies the AN2 locus. Science **244:** 1575–1578.

Golic, K. G., 1994 Local transposition of *P* elements in *Drosophila melanogaster* and recombination between duplicated elements using a site-specific recombinase. Genetics **137:** 551–563.

Golic, K. G., and M. M. Golic, 1996 Engineering the Drosophila genome: chromosome rearrangements by design. Genetics **144:** 1693–1711.

Hakem, R., J. L. de la Pompa, C. Sirard, R. Mo, M. Woo *et al.*, 1996 The tumor suppressor gene Brca1 is required for embryonic cellular proliferation in the mouse. Cell **85:** 1009–1023.

Hill, R. E., J. Favor, B. L. Hogan, C. C. Ton, G. F. Saunders *et al.*, 1991 Mouse small eye results from mutations in a paired-like homeobox-containing gene. Nature **354:** 522–525.

Holdener-Kenny, B., S. K. Sharan and T. Magnuson, 1992 Mouse albino-deletions: from genetics to genes in development. Bioessays **14:** 831–839.

Kaufman, M. H., 1992 *Atlas of Mouse Development*. Academic Press, San Diego.

Khalifa, M. M., P. M. MacLeod and A. M. Duncan, 1993 Additional case of de novo interstitial deletion del(17)(q21.3q23) and expansion of the phenotype. Clin. Genet. **44:** 258–261.

Lakich, D., H. H. J. Kazazian, S. E. Antonarakis and J. Gitschier, 1993 Inversions disrupting the factor VIII gene are a common cause of severe haemophilia A. Nat. Genet. **5:** 236–241.

Levin, M. L., L. G. Shaffer, R. A. Lewis, M. V. Gresik and J. R. Lupski, 1995 Unique de novo interstitial deletion of chromosome 17, del(17) (q23.2q24.3) in a female newborn with multiple congenital anomalies. Am. J. Med. Genet. **55:** 30–32.

Lewandoski, M., and G. R. Martin, 1997 Cre-mediated chromosome loss in mice. Nat. Genet. **17:** 223–225.

Lindsley, D. L., L. Sandler, B. S. Baker, A. T. C. Carpenter, R. E. Denell *et al.*, 1972 Segmental aneuploidy and the genetic gross structure of the Drosophila genome. Genetics **71:** 157–184.

Lupski, J. R., R. M. de Oca-Luna, S. Slaugenhaupt, L. Pentao, V. Guzzetta *et al.*, 1991 DNA duplication associated with Charcot-Marie-Tooth disease type 1A. Cell **26:** 219–232.

Marshall, C. J., 1991 Tumor suppressor genes. Cell **64:** 313–332.

Matzuk, M. M., M. J. Finegold, J. G. Su, A. J. Hsueh and A. Bradley, 1992 Alpha-inhibin is a tumour-suppressor gene with gonadal specificity in mice. Nature **360:** 313–319.

Miki, Y., J. J. Swensen, M. R. Hobbs, B. S. DeHoff, P. R. Rosteck *et al.*, 1995 A physical map encompassing GP2B, EPB3, D17S183, D17S78, D17S1183, and D17S1184. Genomics **25:** 295–297.

Park, J. P., J. B. Moeschler, S. Z. Berg, R. M. Bauer and D. H. Wurster-Hill, 1992 A unique de novo interstitial deletion del(17)(q21.3q23) in a phenotypically abnormal infant. Clin. Genet. **41:** 54–56.

Power, M. A., and P. P. L. Tam, 1993 Onset of gastrulation, morphogenesis and somitogenesis in mouse embryos displaying compensatory growth. Anat. Embryol. **187:** 493–504.

Rabbitts, T. H., 1994 Chromosomal translocations in human cancer. Nature **372:** 143–149.

Ramirez-Solis, R., A. C. Davis and A. Bradley, 1993 Gene targeting in embryonic stem cells. Methods Enzymol. **225:** 855–878.

Ramirez-Solis, R., P. Liu and A. Bradley, 1995 Chromosome engineering in mice. Nature **378:** 720–724.

Rinchik, E. M., 1991 Chemical mutagenesis and fine-structure functional analysis of the mouse genome. Trends Genet. **7:** 15–21.

Rinchik, E. M., and L. B. Russell, 1990 Germ-line deletion mutations in the mouse: Tools for intensive functional and physical mapping of regions of the mammalian genome, pp. 121–159 in *Genome Analysis*, edited by K. E. Davies and S. M. Tilghman. Cold Spring Harbor Laboratory Press, Cold Spring Harbor, NY.

Rinchik, E., L. Flaherty and L. B. Russell, 1993 High-frequency induction of chromosomal rearrangements in mouse germ cells by the chemotherapeutic agent chlorambucil. Bioessays **15:** 831–836.

Robertson, E. J., 1987 Embryo-derived stem cell lines, pp. 71–112 in *Teratocarcinomas and Embryonic Stem Cells—A Practical Approach*, edited by E. J. Robertson. IRL, Oxford.

Sauer, B., and N. Henderson, 1988 Site-specific DNA recombination in mammalian cells by the Cre recombinase of bacteriophage P1. Proc. Natl. Acad. Sci. USA **85:** 5166–5170.

Schuler, G. D., M. S. Boguski, E. A. Stewart, L. D. Stein, G. Gyapay *et al.*, 1996 A gene map of the human genome. Science **274:** 540–546.

Sharan, S. K., M. Morimatsu, U. Albrecht, D. S. Lim, E. Regel *et al.*, 1997 Embryonic lethality and radiation hypersensitivity mediated by Rad51 in mice lacking Brca2. Nature **386:** 804–810.

Shumacher, A., C. Faust and T. Magnuson, 1996 Positional cloning of a global regulator of anterior-posterior patterning in mice. Nature **383:** 250–253.

Sturtevant, A. H., 1926 A crossover reducer in *Drosophila melanogaster* due to inversion of a section of the third chromosome. Biol. Zentralbl **46:** 697–702.

Tassabehji, M., A. P. Read, V. E. Newton, R. Harris, R. Balling *et al.* 1992 Waardenburg's syndrome patients have mutations in the human homologue of the Pax-3 paired box gene. Nature **355:** 635–636.

Thomas, J. W., C. LaMantia and T. Magnuson, 1998 X-ray-induced mutations in mouse embryonic stem cells. Proc. Natl. Acad. Sci. USA **95:** 1114–1119.

Watkins-Chow, D., M. Roller, M. M. Newhouse, A. M. Buchberg and S. A. Camper, 1996 Mouse chromosome *11*. Mamm. Genome **6:** 201–220.

Weinberg, R. A., 1991 Tumor suppressor genes. Science **254:** 1138–1146.

You, Y., R. Bergstrom, M. Klemm, B. Lederman, H. Nelson *et al.*, 1997 Chromosomal deletion complexes in mice by radiation of embryonic stem cells. Nat. Genet. **15:** 285–288.

Zhang, H., P. Hasty and A. Bradley, 1994 Targeting frequency for deletion vectors in embryonic stem cells. Mol. Cell. Biol. **14:** 2404–2410.

Communicating editor: N. A. Jenkins